δ Aromaticity in [Ta3O3]

ARTICLE *in* ANGEWANDTE CHEMIE INTERNATIONAL EDITION · FEBRUARY 2007

Impact Factor: 11.26 · DOI: 10.1002/anie.200700442 · Source: PubMed

DOI: 10.1002/anie.200700442

Aromaticity

δ Aromaticity in $[Ta_3O_3]^-$**

Hua-Jin Zhai, Boris B. Averkiev, Dmitry Yu. Zubarev, Lai-Sheng Wang, and Alexander I. Boldyrev**

The concept of aromaticity was introduced into organic chemistry to describe delocalized π bonding in planar, cyclic, and conjugate molecules possessing $(4n+2)$ π electrons.[1] In recent years, this concept has been advanced into main-group molecules including organometallic compounds with cyclic cores of metal atoms[2] and, in particular, all-metal clusters.[3] It has been shown that main-group clusters may exhibit multiple aromaticity (σ and π), multiple antiaromaticity (σ and π), and conflicting aromaticity (σ aromaticity and π antiaromaticity or σ antiaromaticity and π aromaticity).[4–6] Here, we report experimental and theoretical evidence of δ aromaticity, which is only possible in transition-metal systems. It is discovered in the $[Ta_3O_3]^-$ cluster through combined photoelectron spectroscopy and ab initio studies. Well-resolved low-lying electronic transitions are observed in the photoelectron spectra of $[Ta_3O_3]^-$ and are compared with ab initio calculations, which show that the $[Ta_3O_3]^-$ cluster has a planar D_{3h} triangular structure. Chemical-bonding analyses reveal that among the five valence molecular orbitals involved in the multicenter metal–metal bonding, there is a completely bonding δ and π orbital formed from the 5d atomic orbitals of Ta. The totally delocalized multicenter δ bond renders δ aromaticity for $[Ta_3O_3]^-$ and represents a new mode of chemical bonding. $[Ta_3O_3]^-$ is the first δ-aromatic molecule confirmed experimentally and theoretically, which suggests that δ aromaticity may exist in many multinuclear, low-oxidation-state transition-metal compounds.

In 1964, Cotton and co-workers published a milestone work on $K_2[Re_2Cl_8]\cdot 2H_2O$,[7] in which they showed the presence of a new type of chemical bond—a δ bond between the two Re atoms. Since then, a branch of inorganic chemistry has been developed that involves multiple metal–metal bonding[8] with bond orders higher than three, the maximum allowed for main-group systems. Power and co-workers recently reported the synthesis of a Cr_2 compound with a quintuple bond ($\sigma^2\pi^4\delta^4$) between the two Cr atoms.[9] This work, along with recent quantum chemical studies of multiple bonds in U_2 and $[Re_2Cl_8]^{2-}$,[10] has generated renewed interest in multiple metal–metal bonding.[11–13] The presence of δ bonds between two transition-metal atoms suggests that multicenter transition-metal species with a completely delocalized cyclic δ bond may exist, thus raising the possibility of δ aromaticity analogous to π or σ aromaticity in main-group systems. We have been interested in understanding the electronic structure and chemical bonding of early transition-metal oxide clusters as a function of size and composition, and in using them as potential molecular models for oxide catalysts.[14–16] During our investigation of tantalum oxide clusters, we found the presence of δ aromaticity in the $[Ta_3O_3]^-$ cluster, in which each Ta atom is in a low oxidation state of Ta^{II} and still possesses three electrons for Ta–Ta bonding.

The experiment was conducted by using a magnetic-bottle-type photoelectron spectroscopy apparatus equipped with a laser vaporization cluster source.[17] $[Ta_mO_n]^-$ clusters with various compositions were produced by laser vaporization of a pure tantalum disk target in the presence of a helium carrier gas seeded with O_2, and were size-separated by time-of-flight mass spectrometry. The $[Ta_3O_3]^-$ species was mass-selected and decelerated before photodetachment by a pulsed laser beam. Photoelectron spectra were obtained at two relatively high photon energies, 193 nm (6.424 eV) and 157 nm (7.866 eV), to guarantee access to all valence electronic transitions (Figure 1). Three well-resolved bands (X, A, and B) were observed at the lower-binding-energy side. The X band is much more intense and shows a discernible splitting at 193 nm (Figure 1a). Surprisingly, no well-defined electronic transitions were observed beyond 3.7 eV, where continuous signals were present, probably as a result of multielectron transitions. The vertical detachment energies (VDEs) of the observed transitions at the low-binding-energy side are given in Table 1, where they are compared with theoretical calculations by two different methods.

[*] Dr. H. J. Zhai, Prof. Dr. L. S. Wang
Department of Physics
Washington State University
2710 University Drive, Richland, WA 99354 (USA)
and
Chemical & Materials Sciences Division
Pacific Northwest National Laboratory
MS K8–88, P.O. Box 999, Richland, WA 99352 (USA)
Fax: (+1) 509-376-6066
E-mail: ls.wang@pnl.gov
B. B. Averkiev, D. Y. Zubarev, Prof. Dr. A. I. Boldyrev
Department of Chemistry and Biochemistry
Utah State University
Logan, UT 84322 (USA)
Fax: (+1) 435-797-3390
E-mail: boldyrev@cc.usu.edu

[**] The theoretical work done at Utah was supported by the donors of the Petroleum Research Fund, administered by the American Chemical Society and the National Science Foundation. The experimental work done at Washington was supported by the Chemical Sciences, Geosciences, and Biosciences Division, Office of Basic Energy Sciences, U.S. Department of Energy (DOE) under the catalysis center program and was performed at the EMSL, a national scientific user facility sponsored by the DOE's Office of Biological and Environmental Research and located at Pacific Northwest National Laboratory, operated for the DOE by Battelle.

Supporting information for this article is available on the WWW under http://www.angewandte.org or from the author.

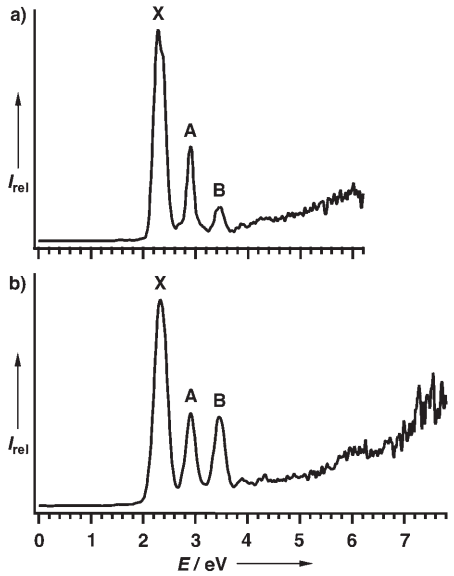

Figure 1. Photoelectron spectra of $[Ta_3O_3]^-$. a) 193 nm (6.424 eV); b) 157 nm (7.866 eV).

Table 1: Experimental VDEs [eV] for $[Ta_3O_3]^-$ compared with those calculated for the D_{3h} global minimum.

	VDE (exp.)	Final state and configuration	VDE (B3LYP)[a]	VDE (B3PW91)[a]
X	2.25 ± 0.03[b]	$^2E'$ ($3a_1'^2 2a_2''^2 4a_1'^2 4e'^3$)	2.27	2.25
A	2.89 ± 0.02	$^2A_1'$ ($3a_1'^2 2a_2''^2 4a_1'^1 4e'^4$)	2.93	2.96
B	3.44 ± 0.03	$^2A_2''$ ($3a_1'^2 2a_2''^1 4a_1'^2 4e'^4$)	3.27	3.36

[a] Using the Ta/Stuttgart + 2f1g/O/aug-cc-pvTZ basis set. [b] The adiabatic electron-detachment energy was measured to be (2.22 ± 0.03) eV.

We initially performed an extensive search for the $[Ta_3O_3]^-$ global minimum for the singlet, triplet, and quintet states at the B3LYP/LANL2DZ level of theory, and then recalculated the global minimum structure and the three lowest isomers at three other levels of theory (see the Supporting Information for references, details of theoretical calculations, and more theoretical results). We found that the $[Ta_3O_3]^-$ global minimum has a perfect D_{3h} ($^1A_1'$) planar triangular structure I (Figure 2). The closest isomer II is 6.6 (B3LYP/Ta/Stuttgart + 2f1g/O/aug-cc-pvTZ) and 1.7 kcal mol^{-1} (B3PW91/Ta/Stuttgart + 2f1g/O/aug-cc-pvTZ) higher in energy than the D_{3h} ground state. The theoretical VDEs of the global minimum at the two highest levels of theory are compared with the experimental data in Table 1. One can see that the calculated VDEs for the global minimum structure I agree well with the experimental results, whereas those for the three low-lying isomers (see the Supporting Information) are completely off, thus lending considerable credence to the theoretical methods and the D_{3h} structure for $[Ta_3O_3]^-$. The highest occupied molecular orbital (HOMO, 4e′) of the D_{3h} $[Ta_3O_3]^-$ is doubly degenerate, consistent with the intense X band observed experimentally. The splitting of the X band could be a consequence of either a Jahn–Teller effect or spin–orbit coupling.

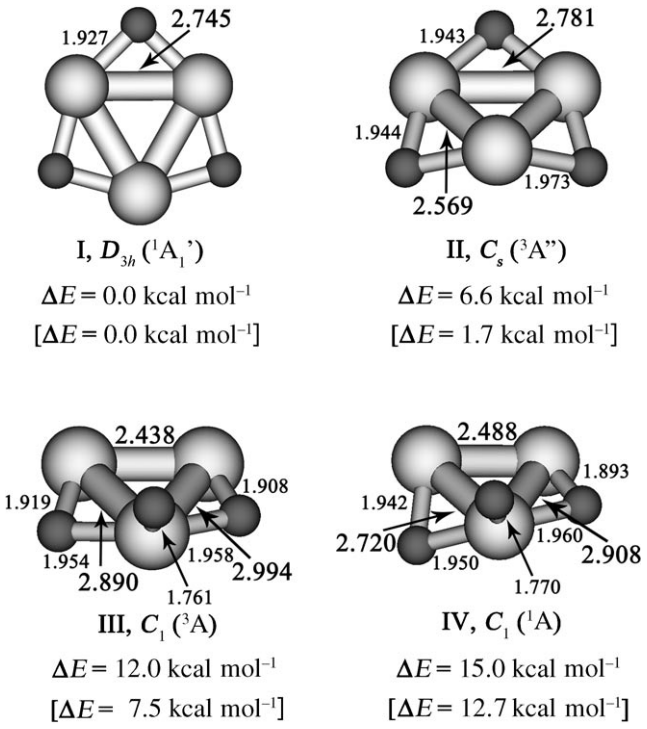

Figure 2. Optimized structures for the global minimum of $[Ta_3O_3]^-$ (D_{3h}, $^1A_1'$) and selected low-lying isomers. The relative energies ΔE_{total} [kcal mol^{-1}] and interatomic distances [Å] were calculated at the B3LYP/Ta/Stuttgart + 2f1g/O/aug-cc-pvTZ level of theory (ΔE_{total} at the B3PW91/Ta/Stuttgart + 2f1g/O/aug-cc-pvTZ level is shown in brackets).

To help understand the structure and bonding in $[Ta_3O_3]^-$ we performed a detailed molecular orbital (MO) analysis. Out of the 34 valence electrons in $[Ta_3O_3]^-$, 24 belong to either pure oxygen lone pairs or those polarized towards Ta (responsible for the covalent contributions to Ta–O bonding). The remaining ten valence electrons are primarily Ta-based and are involved in direct metal–metal bonding (Figure 3). Among the five MOs, three are responsible for σ bonding of the triangular Ta_3 framework. They include the partially bonding/antibonding doubly degenerate 4e′ HOMO and the completely bonding $3a_1'$ HOMO-3. The antibonding nature of the HOMO significantly reduces the σ-bonding contribution to the Ta_3 framework.[18] In the $[Ta_3O_3]^-$ anion, the HOMO-2 ($2a_2''$) is a completely bonding π orbital composed primarily of the 5d orbitals of Ta, thus giving rise to π-aromatic character according to the ($4n$+2) Hückel rule for π aromaticity.[19]

The most interesting MO is HOMO-1 ($4a_1'$), which is a completely bonding orbital that comes mainly from the overlap of the d_{z^2} orbital on each Ta atom. This orbital has the "appearance" of a π orbital with major overlaps above and below the molecular plane, but it is not a π-type MO because it is symmetric with respect to the molecular plane. However, perpendicular to the molecular C_3 axis this MO has two nodal surfaces, and thus it is a δ orbital.[20] In fact, a similar δ-bonding MO exists in the recently synthesized quintuple-bond Cr_2 complex,[9] in which it is a two-center bond formed from a d_{z^2} orbital on each Cr atom.[13] Analogous to the

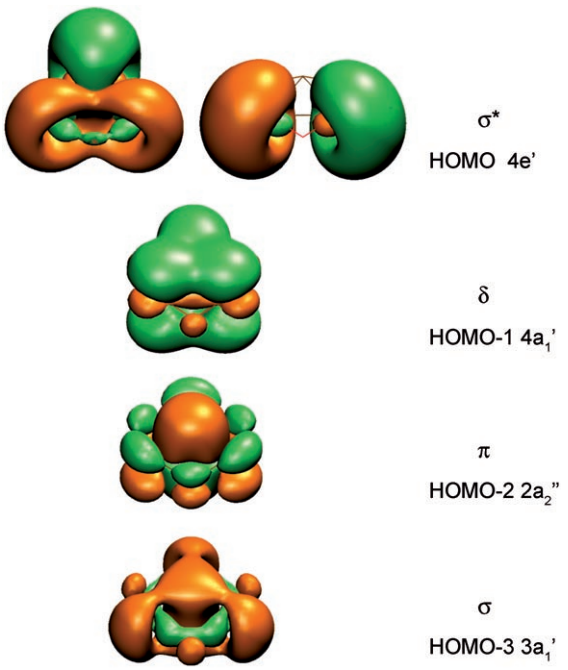

Figure 3. The five valence MOs responsible for the metal–metal bonding in $[Ta_3O_3]^-$ (D_{3h}, $^1A_1'$).

circularly delocalized π MO over three carbon atoms, which renders $[C_3H_3]^+$ π-aromatic,[6] the circular delocalization and the bonding nature of the $4a_1'$ MO give rise to δ aromaticity in $[Ta_3O_3]^-$, which is also consistent with the $(4n+2)$ Hückel rule.[19] In the $[Ta_3O_3]^-$ cluster, the δ MO is a three-center bond, but similar types of MOs are possible in planar tetraatomic, pentaatomic, or larger transition-metal systems.

Therefore, the $[Ta_3O_3]^-$ cluster exhibits an unprecedented multiple (δ and π) aromaticity, which is responsible for the metal–metal bonding and the perfect triangular Ta_3 framework. The stability of the Ta_3 triangular kernel can be seen in all the low-lying isomers of $[Ta_3O_3]^-$ (Figure 2 and the Supporting Information), which differ only in the coordination of the oxygen atoms to the aromatic Ta_3 framework. Notably, the energy ordering of σ (HOMO-3) < π (HOMO-2) < δ (HOMO-1) (Table 1 and Figure 3) indicates that the strength of the metal–metal bonding increases from δ to π to σ, in agreement with the intuitive expectation that σ-type overlap is greater than π-type overlap, and that δ-type overlap is the weakest, as is also the case in the multiple bonding of diatomic transition-metal compounds including the classical $[Re_2Cl_8]^{2-}$.[7–13] Despite the expected weaker overlap in the δ MO, it makes important contributions to the overall metal–metal bonding, as shown in the quintuple bonds in the new Cr_2 complex[9,11–13] or in the U_2 dimer.[10] The three-center delocalization in the aromatic δ MO in $[Ta_3O_3]^-$ is expected to provide even more bonding contributions than in the cases of the metal dimers, even though it is difficult to quantify them. The three-center delocalization in the aromatic $[W_3O_9]^{2-}$ ion that results from a d–d σ bond was estimated previously to provide about 1 eV additional resonance energy, similar to that estimated for benzene.[21]

Aromaticity in transition-metal systems has been discussed in the literature,[4,5,21–30] particularly since the discovery of aromaticity in all-metal clusters.[3] King[22] and Li[23] have considered aromaticity in transition-metal oxides as a result of metal–metal interactions through M-O-M bridges. The $[Hg_4]^{6-}$ cluster, which is a building block of the $[Na_3Hg_2]$ amalgam, has been shown by Kuznetsov et al.[24] to be aromatic and similar to the all-metal $[Al_4]^{2-}$ unit.[3] Tsipis et al.[25,26] explained the planar structure of cyclic coinage-metal hydrides on the basis of their aromatic character. Aromaticity in square-planar coinage-metal clusters was discussed by Wannere et al.[27] and Lin et al.,[28] and Alexandrova et al.[29] suggested the presence of aromaticity in the $[Cu_3C_4]^-$ cluster. Datta et al.[30] used d-orbital aromaticity to explain the metal-ring structure in tiara nickel thiolates. Recently, Huang et al.[21] demonstrated the presence of d-orbital aromaticity in the 4d and 5d transition-metal-oxide clusters $[Mo_3O_9]^{2-}$ and $[W_3O_9]^{2-}$. The claim of d-orbital aromaticity in the square-planar coinage-metal clusters[27] was questioned by Lin et al.,[28] who showed that the completely filled d orbitals do not play any significant role in the bonding in these clusters. Instead, aromaticity in these systems comes primarily from σ-bonding interactions of the valence s electrons. Thus, today the $[Mo_3O_9]^{2-}$ and $[W_3O_9]^{2-}$ clusters are the only examples in which aromaticity comes from d-bonding interactions, albeit with σ character.[21]

In the $[Ta_3O_3]^-$ cluster, we have found two new types of d-bonding interactions that lead to π and δ aromaticity. The δ aromaticity in this cluster is a new mode of chemical bonding that can only occur in multinuclear transition-metal systems. The current finding suggests that δ aromaticity may exist in many cyclic transition-metal systems containing metal atoms in low oxidation states. The next challenge is to find φ aromaticity, which may occur in multinuclear and cyclic f-metal systems.

Received: January 31, 2007
Published online: April 30, 2007

Keywords: ab initio calculations · aromaticity · cluster compounds · metal–metal interactions · photoelectron spectroscopy

[1] V. I. Minkin, M. N. Glukhovtsev, B. Ya. Simkin, *Aromaticity and Antiaromaticity*, Wiley, New York, **1994**; see also special issues: *Chem. Rev.* **2001**, *101*(5) and *Chem. Rev.* **2005**, *105*(10).
[2] G. H. Robinson, *Acc. Chem. Res.* **1999**, *32*, 773.
[3] X. Li, A. E. Kuznetsov, H. F. Zhang, A. I. Boldyrev, L. S. Wang, *Science* **2001**, *291*, 859.
[4] A. I. Boldyrev, L. S. Wang, *Chem. Rev.* **2005**, *105*, 3716, and references therein.
[5] C. A. Tsipis, *Coord. Chem. Rev.* **2005**, *249*, 2740.
[6] M. Hofmann, A. Berndt, *Heteroat. Chem.* **2006**, *17*, 224.
[7] F. A. Cotton, N. F. Curtis, C. B. Harris, B. F. G. Johnson, S. J. Lippard, J. T. Mague, W. R. Robinson, J. S. Wood, *Science* **1964**, *145*, 1305.
[8] F. A. Cotton, C. A. Murillo, R. A. Walton, *Multiple Bonds Between Metal Atoms*, 3rd ed., Springer, New York, **2005**.
[9] T. Nguyen, A. D. Sutton, M. Brynda, J. C. Fettiger, G. J. Long, P. P. Power, *Science* **2005**, *310*, 844.

[10] a) L. Gagliardi, O. B. Roos, *Nature* **2005**, *433*, 848; b) L. Gagliardi, O. B. Roos, *Inorg. Chem.* **2003**, *42*, 1599; c) K. Saito, Y. Nakao, H. Sato, S. Sakaki, *J. Phys. Chem. A* **2006**, *110*, 9710.
[11] G. Frenking, *Science* **2005**, *310*, 796.
[12] U. Radius, F. Breher, *Angew. Chem.* **2006**, *118*, 3072; *Angew. Chem. Int. Ed.* **2006**, *45*, 3006.
[13] M. Brynda, L. Gagliardi, P.-O. Widmark, P. P. Power, B. O. Roos, *Angew. Chem.* **2006**, *118*, 3888; *Angew. Chem. Int. Ed.* **2006**, *45*, 3804.
[14] H. J. Zhai, B. Kiran, L. F. Cui, X. Li, D. A. Dixon, L. S. Wang, *J. Am. Chem. Soc.* **2004**, *126*, 16134.
[15] X. Huang, H. J. Zhai, J. Li, L. S. Wang, *J. Phys. Chem. A* **2006**, *110*, 85.
[16] X. Huang, H. J. Zhai, T. Waters, J. Li, L. S. Wang, *Angew. Chem.* **2006**, *118*, 673; *Angew. Chem. Int. Ed.* **2006**, *45*, 657.
[17] L. S. Wang, H. Wu in *Advances in Metal and Semiconductor Clusters. IV. Cluster Materials* (Ed.: M. A. Duncan), JAI, Greenwich, CT, **1998**, pp. 299–343.
[18] If the HOMO (4e′) and the HOMO-3 ($3a_1'$) were composed of the same s–d hybrid functions they would cancel each other, thus resulting in negligible metal–metal σ bonding. However, the hybridization in the 4e′ and $3a_1'$ orbitals is somewhat different. Therefore, we cannot rule out some σ-bonding contribution in the Ta_3 framework; that is, there should be some σ-aromatic character in $[Ta_3O_3]^-$.
[19] In the case of multiple aromaticity, the $(4n+2)$ counting rule should be applied separately for each type of aromaticity encountered in a particular planar system, that is, separately for σ-, π-, δ-, and ϕ-type MOs.[4]
[20] Strictly speaking, the σ, π, δ, and ϕ notations for MOs are only appropriate for linear systems, where they are irreducible representations of the $C_{\infty v}$ and $D_{\infty h}$ point groups. However, it is customary in chemistry to use π notation in planar molecules for MOs that are formed by the p_z atomic orbitals and are perpendicular to the molecular plane, even though they do not belong to the π-irreducible representation. For example, the orbitals responsible for the aromaticity in the prototypical aromatic molecule C_6H_6 are called π orbitals. Following this tradition, one can introduce δ- or ϕ-type MOs in planar molecules formed from appropriate atomic orbitals.
[21] X. Huang, H. J. Zhai, B. Kiran, L. S. Wang, *Angew. Chem.* **2005**, *117*, 7417; *Angew. Chem. Int. Ed.* **2005**, *44*, 7251.
[22] R. B. King, *Inorg. Chem.* **1991**, *30*, 4437.
[23] J. Li, *J. Cluster Sci.* **2002**, *13*, 137.
[24] A. E. Kuznetsov, J. D. Corbett, L. S. Wang, A. I. Boldyrev, *Angew. Chem.* **2001**, *113*, 3473; *Angew. Chem. Int. Ed.* **2001**, *40*, 3369.
[25] A. C. Tsipis, C. A. Tsipis, *J. Am. Chem. Soc.* **2003**, *125*, 1136.
[26] C. A. Tsipis, E. E. Karagiannis, P. F. Kladou, A. C. Tsipis, *J. Am. Chem. Soc.* **2004**, *126*, 12916.
[27] C. S. Wannere, C. Corminboeuf, Z.-X. Wang, M. D. Wodrich, R. B. King, P. von R. Schleyer, *J. Am. Chem. Soc.* **2005**, *127*, 5701.
[28] Y.-C. Lin, D. Sundholm, J. Juselius, L. F. Cui, H. J. Zhai, L. S. Wang, *J. Phys. Chem. A* **2006**, *110*, 4244.
[29] A. N. Alexandrova, A. I. Boldyrev, H. J. Zhai, L. S. Wang, *J. Phys. Chem. A* **2005**, *109*, 562.
[30] A. Datta, N. S. John, G. U. Kulkarni, S. K. Pati, *J. Phys. Chem. A* **2005**, *109*, 11647.

Angewandte Chemie
Eine Zeitschrift der Gesellschaft Deutscher Chemiker

Supporting Information

69451 Weinheim, Germany

δ-Aromaticity in $Ta_3O_3^-$: A New Mode of Chemical Bonding

Hua-Jin Zhai, Boris B. Averkiev, Dmitry Yu. Zubarev, Lai-Sheng Wang, and Alexander I. Boldyrev

Theoretical Methods:

The G03 quantum chemical package was used for all the calculations.[1] The initial search for the $Ta_3O_3^-$ global minimum structure was performed for singlet, triplet and quintet states at the B3LYP[2]/LANL2DZ[3] level of theory. We recalculated the global minimum structure and the three lowest isomers with the B3PW91/LANLDZ method and using the Stuttgart relativistic small core basis set and efficient core potential[4a] augmented with 2f and 1g functions[4b] (Stuttgart+2f1g) on Ta atoms and aug-cc-pvTZ[5] (AVTZ) basis set on O atoms at the B3LYP and B3PW91 methods. We found that during G03 computations it was necessary to use the ultrafine integration grid to achieve reliable convergence during computations. All four levels of theory give the same triangular global minimum structure. Hartree-Fock molecular orbitals were visualized using the VMD software.[6]

Because there is a low-lying triplet isomer (at B3PW91/Ta/Stuttgart+2f1g/O/ aug-cc-pvTZ) we performed the test of stability of the closed-shell wave-function at the ROB3LYP/ Ta/Stuttgart+2f1g/O/aug-cc-pvTZ level of theory. We found that there is a small RHF → UHF instability with the spin-restricted energy (–397.050037 au) being slightly higher than the spin-unrestricted energy (–397.050108 au). We believe that this instability cannot affect our results. However we performed additional testes of possible open-shell singlet nature of our ground electronic state. We calculated first ten singlet excited states from the D_{3h}, $^1A_1$' global minimum using TD- B3LYP/Ta/Stuttgart+2f1g/O/aug-cc-pvTZ as well as from additional 15 geometries

distorted along the two independent parameters within D_{3h} symmetry. The lowest singlet excited state for the optimized D_{3h}, $^1A_1$' state was found to be 1.36 eV above the ground state. For all other distorted geometries we found that the first singlet excited state is also higher in energy.

To further test the applicability of the single-configurational methods and the possible open-shell singlet nature of the global minimum ground electronic state we performed a single point calculation at the multi-configuration self-consistent-field (CASSCF) level of theory with 12 active electrons and 12 active orbitals and found that the Hartree-Fock configuration is dominant (C_{HF} = 0.861) among 427,350 configurations in the CASSCF expansion (all other configurations have coefficient less than 0.16) using the Ta/Stuttgart+2f1g/O/aug-cc-pvTZ basis set. Here C_{HF} is still close to the 0.9 value, which is usually accepted as the threshold for the applicability of the one-electron approximation. We then calculated the VDEs from the valence orbitals of $Ta_3O_3^-$ using ROB3LYP/Ta/Stuttgart+2f1g/O/ aug-pvTZ and ROPW91/Ta/ Stuttgart+2f1g/O/aug-pvTZ levels of theory.

It was important to use restricted open shell DFT methods for calculations of vertical electron detachment energies, because of high spin-contamination in the unrestricted open shell DFT calculations. We were only able to calculate the VDEs from the first three valence orbitals (4e', $4a_1$', and $2a_2$"), which all have different symmetries. VDEs for higher binding energy orbitals with the same symmetries could not be computed using the current methods.

References:

[1] Gaussian 03. (revision A.1). M. J. Frisch, G. W. Trucks, H. B. Schlegel, G. E. Scuseria, M. A. Robb, J. R. Cheeseman, J. A. Montgomery, Jr., T. Vreven, K. N. Kudin, J. C. Burant, J. M. Millam, S. S. Iyengar, J. Tomasi, V. Barone, B. Mennucci, M. Cossi, G. Scalmani, N. Rega, G. A. Petersson, H. Nakatsuji, M. Hada, M. Ehara, K. Toyota, R. Fukuda, J. Hasegawa, M. Ishida, T. Nakajima, Y.

Honda, O. Kitao, H. Nakai, M. Klene, X. Li, J. E. Knox, H. P. Hratchian, J. B. Cross, V. Bakken, C. Adamo, J. Jaramillo, R. Gomperts, R. E. Stratmann, O. Yazyev, A. J. Austin, R. Cammi, C. Pomelli, J. W. Ochterski, P. Y. Ayala, K. Morokuma, G. A. Voth, P. Salvador, J. J. Dannenberg, V. G. Zakrzewski, S. Dapprich, A. D. Daniels, M. C. Strain, O. Farkas, D. K. Malick, A. D. Rabuck, K. Raghavachari, J. B. Foresman, J. V. Ortiz, Q. Cui, A. G. Baboul, S. Clifford, J. Cioslowski, B. B. Stefanov, G. Liu, A. Liashenko, P. Piskorz, I. Komaromi, R. L. Martin, D. J. Fox, T. Keith, M. A. Al-Laham, C. Y. Peng, A. Nanayakkara, M. Challacombe, P. M. W. Gill, B. Johnson, W. Chen, M. W. Wong, C. Gonzalez, J. A. Pople, (Gaussian, Inc., Pittsburgh PA, 2003).

[2] (a) R. G. Parr, W. Yang, *Density-Functional Theory of Atoms and Molecules*, Oxford Univ. Press, Oxford, 1989. (b) A. D. Becke, *J. Chem. Phys*. **1993**, *98*, 5648. (c) J. P. Perdew, J. A. Chevary, S. H. Vosko, K. A. Jackson, M. R. Pederson, D. J., Singh, C. Fiolhais, *Phys. Rev. B* **1992**, *46*, 6671.

[3] P. J. Hay, W. R. Wadt*, J. Chem. Phys*. **1985**, *82*, 299.

[4] (a) M. Dolg, U. Wedig, H. Stoll, H. Preuss, *J. Chem. Phys*. **1987**, *86*, 866. (b) J. M. L. Martin, A. Sundermann, *J. Chem. Phys*. **2001**, *114*, 3408.

[5] (a) T. H. Dunning, *J. Chem. Phys.* **1989**, *90*, 1007. (b) D. E. Woon, T. H. Dunning, *J. Chem. Phys.* **1993**, *98*, 1358. (c) R. A. Kendall, T. H. Dunning, R. J. Harrison, *J. Chem. Phys*. **1992**, *96*, 6796. (d) K. A. Peterson, D. E. Woon, T. H. Dunning, *J. Chem. Phys.* **1994**, *100*, 7410. (e) A. K. Wilson, T. van Mourik, T. H. Dunning, *J. Mol. Struct. (Theochem)* **1996**, *388*, 339. (f) E. R. Davidson, *Chem. Phys*. *Lett.* **1996**, *260*, 514.

[6] VMD (Visual Molecular Dynamics). W. Humphrey, A. Dalke, K. Schulten, *J. Molec. Graphics* **1996**, *14*, 33.

Table S1: Experimental and theoretical vertical electron detachment energies (VDE) low-lying isomers for $Ta_3O_3^-$ in eV (see Figure 2).

Structure	Final State and Configuration	VDE (B3LYP)[a]	VDE (B3PW91)[a]
II	$^2A'$ ($9a'^2 6a''^2 10a'^2 11a'^1$)	1.65	1.62
	$^2A''$ ($9a'^2 6a''^2 10a'^2 7a''^1$)	1.78	1.76
	$^4A''$ ($9a'^2 6a''^2 10a'^1 7a''^1 11a'^1$)	1.95	1.90
	$^4A'$ ($9a'^2 6a''^1 10a'^2 7a''^1 11a'^1$)	2.37	2.46
	$^4A''$ ($9a'^1 6a''^2 10a'^2 7a''^1 11a'^1$)	2.68	2.72
III	^2A ($14a^2 15a^2 16a^2 17a^1$)	1.90	1.86
	^4A ($14a^2 15a^2 16a^1 17a^1 18a^1$)	2.15	2.10
	^4A ($14a^2 15a^1 16a^2 17a^1 18a^1$)	2.92	2.99
	^4A ($14a^1 15a^2 16a^2 17a^1 18a^1$)	3.15	3.16
IV	^2A ($14a^2 15a^2 16a^2 17a^1$)	1.67	1.54
	^2A ($14a^2 15a^2 16a^1 17a^2$)	2.62	2.61
	^2A ($14a^2 15a^1 16a^2 17a^2$)	2.74	2.79
	^2A ($14a^2 15a^1 16a^2 17a^2$)	2.78	2.92
	^2A ($14a^1 15a^2 16a^2 17a^2$)	3.33	3.35

[a] Using the Ta/Stuttgartt+2f1g/O/aug-cc-pvTZ basis set.

Table S2: Molecular properties of $Ta_3O_3^-$ D_{3h} ($^1A_1$') species.

Property	B3LYP/ LANL2DZ	B3LYP/ Ta/Stuttgart+2f1g/ O/aug-cc-pvTZ	B3PW91/ LANL2DZ	B3PW91/ Ta/Stuttgart+2f1g/ O/aug-cc-pvTZ
E_{total}, eV	-399.300548	-397.050037	-399.288444	-397.054220
ZPE, kcal/mol	6.26	6.29	6.21	6.29
R (Ta-Ta), Å	2.765	2.745	2.742	2.719
R (Ta-O), Å	1.938	1.927	1.932	1.918
$\omega_1(a_1')$, cm^{-1}	208 (0.0)[a]	221 (0.0)[a]	211 (0.0)[a]	227 (0.0)[a]
$\omega_2(a_1')$, cm^{-1}	686 (0.0)	694 (0.0)	692 (0.0)	704 (0.0)
$\omega_3(a_2')$, cm^{-1}	371 (0.0)	372 (0.0)	369 (0.0)	374 (0.0)
$\omega_4(a_2'')$, cm^{-1}	134 (0.0)	116 (0.8)	112 (0.0)	96 (1.0)
$\omega_5(e')$, cm^{-1}	143 (4.3)	151 (3.4)	147 (4.7)	155 (3.6)
$\omega_6(e')$, cm^{-1}	606 (8.8)	620 (18.5)	607 (7.3)	627 (16.4)
$\omega_7(e')$, cm^{-1}	667 (72.8)	669 (53.3)	675 (75.9)	680 (51.0)
$\omega_8(e'')$, cm^{-1}	74 (0.0)	59 (0.0)	51 (0.0)	39 (0.0)

[a]Infrared intensities (km/mol) are given in parenthesis

Cartesian coordinates (Å) of alternative $Ta_3O_3^-$ structures at B3LYP/LANL2DZ:

	X	Y	Z
Structure I			
Ta	0.000000	1.584618	0.000000
Ta	1.372320	-0.792309	0.000000
Ta	-1.372320	-0.792309	0.000000
O	-1.857751	1.072573	0.000000
O	0.000000	-2.145146	0.000000
O	1.857751	1.072573	0.000000
Structure II			
Ta	-0.239987	-0.677040	-1.416577
Ta	-0.239987	-0.677040	1.416577
Ta	0.558238	1.307734	0.000000
O	-0.239987	1.223603	1.839239
O	-0.234177	-2.024306	0.000000
O	-0.239987	1.223603	-1.839239
Structure III			
Ta	-1.642215	-0.120903	-0.118157
Ta	1.212557	-1.128379	0.020533
Ta	0.919815	1.277349	0.061698
O	-2.992295	-0.126206	1.031202
O	-0.587665	-1.775167	-0.189833
O	-0.892722	1.645256	-0.513549
Structure IV			
Ta	-1.503063	-0.322252	-0.105986
Ta	1.353209	-0.967995	0.003059
Ta	0.603764	1.378469	0.099916
O	-2.807699	-0.247631	1.103603
O	-0.317944	-1.894781	-0.052923
O	-1.016287	1.337394	-1.023199
Structure V			
Ta	0.000000	0.000000	1.564447
Ta	0.000000	1.489977	-0.791073
Ta	0.000000	-1.489977	-0.791073
O	0.000000	1.909713	1.110056
O	0.000000	-1.909713	1.110056
O	0.000000	0.000000	-2.058602
Structure VI			
Ta	1.171067	-1.037276	0.109421
Ta	0.604860	1.336480	0.065808
Ta	-1.621815	-0.189259	-0.181400
O	-2.962086	0.387298	0.843473
O	-0.570427	-1.858147	0.016656
O	2.126244	0.467608	-0.803812
Structure VII			

```
  Ta   1.194095  -1.025362   0.077556
  Ta   0.485713   1.381297   0.075447
  Ta  -1.542725  -0.264975  -0.206576
   O  -2.803291   0.362420   0.887791
   O  -0.503191  -1.870939   0.304323
   O   2.055595   0.678512  -0.703261

Structure VIII
  Ta  -1.166888  -1.129739   0.044735
  Ta  -0.530306   1.483094  -0.081751
  Ta   1.561477  -0.216641  -0.110874
   O   2.763619   0.094942   1.164563
   O   0.497361  -1.882332  -0.469793
   O  -2.022564   0.539868   0.654727

Structure IX
  Ta   0.146223   1.669426   0.000000
  Ta  -0.143058  -1.073105   1.217001
  Ta  -0.143058  -1.073105  -1.217001
   O   1.562628   2.730768   0.000000
   O  -0.143058   0.809943   1.735180
   O  -0.143058   0.809943  -1.735180

Structure X
  Ta  -0.954227  -1.198790   0.053323
  Ta  -0.741715   1.372560  -0.127047
  Ta   1.517426  -0.073169  -0.059095
   O   2.841622   0.585972   0.958784
   O   0.678978  -1.807140  -0.709116
   O  -1.891642   0.303187   0.962310

Structure XI
  Ta  -0.000723  -0.853696   1.351214
  Ta   0.071561   1.711908   0.000000
  Ta  -0.000723  -0.853696  -1.351214
   O  -0.000723   1.040457   1.821698
   O  -0.638355  -2.122123   0.000000
   O  -0.000723   1.040457  -1.821698

Structure XII
  Ta   1.355226  -0.988819   0.031087
  Ta   0.352608   1.482825  -0.031761
  Ta  -1.580975  -0.368608  -0.116722
   O  -3.028235   0.026680   0.847674
   O  -0.299445  -1.928000  -0.046848
   O   2.170091   0.757061   0.270405
```

Figure S1. Low-lying isomers of $Ta_3O_3^-$. Relative energies (kcal/mol) are given at the B3LYP/LANL2DZ.